

Results & Discussion

Role of Poly(ADP-Ribose) Polymerase (PARP) in oxidative stress induced cell death in *D. discoideum*

3.1. INTRODUCTION

Programmed cell death (PCD) occurs as a normal component of the development of multicellular eukaryotes. In most of the models studied so far, PCD follows an apoptotic pattern; however, other PCD morphological types have also been described. Cell death can occur in a programmed manner independent of caspases, and paraptosis is one such type (Sperandio *et al.*, 2000). Paraptosis is characterized by cytoplasmic vacuolization, mitochondrial swelling and absence of caspase activation as well as oligonucleosomal DNA fragmentation (Sperandio *et al.*, 2000; Wyllie and Golstein, 2001; Katoch *et al.*, 2002). Interestingly, both types of programmed cell death i.e., apoptotic and paraptotic cell death are seen in mammalian cells. Unlike apoptotic cell death, the biochemical and molecular aspects of paraptotic cell death are yet to be fully understood. Paraptosis has been described to be mediated by mitogen activated protein kinases (Sperandio *et al.*, 2004) and can be triggered by the Tumour Necrosis Factor (TNF) receptor family member TAJ/TROY (Wang *et al.*, 2003), the insulin like growth factor I receptor (Sperandio *et al.*, 2004), epidermal growth factor (Fombonne *et al.*, 2006) and poly(ADP-ribose) polymerase (PARP) activation *via* DNA damage (Haince *et al.*, 2007; Lepretre *et al.*, 2009).

Cell death can be induced by a number of agents including reactive oxygen species (ROS) (Hasnain *et al.*, 1999; Mohan *et al.*, 2003; Sah *et al.*, 1999). ROS in addition to other apoptotic stimuli activate PARP, a nuclear enzyme that has various physiological functions (Burkley, 2001; de Murcia *et al.*, 1994; Lautier *et al.*, 1993; Shall and de Murcia, 2000). Activated PARP cleaves its substrate NAD⁺ and transfers ADP-ribose units to several target proteins including itself (Burkley, 2001; de Murcia *et al.*, 1994; Shall and de Murcia, 2000; Smulson *et al.*, 2000). PARP activation /over activation may result in apoptotic /paraptotic /necrotic cell death, wherein the type of cell death depends on the experimental conditions such as the cell type as well as nature of the stimulus (Virag, 2006). PARP mediated necrotic cell death is reported during ischemia reperfusion injury (Eliasson *et al.*, 1997; Endres *et al.*, 1997), inflammatory

injury and reactive oxygen species induced injury (Szabo and Dawson, 1998). However, the role of PARP in paraptotic cell death is yet to be fully understood. Downstream to PARP activation, a cascade of events occurs where in, mitochondria are known to play a central role (Hong *et al.*, 2004). Mitochondrial proteins such as apoptosis inducing factor (AIF) (Loeffler *et al.*, 2001; Joza *et al.*, 2001; Susin *et al.*, 1999) and endonuclease G have been implicated in the execution of paraptotic cell death (Wang *et al.*, 2004).

D. discoideum, a unicellular eukaryote exhibits multicellularity upon starvation (Raper, 1984) and has nine potential PARP genes (Otto *et al.*, 2005), while yeast which lacks PARP (Perkins *et al.*, 2001), does not show multicellularity. Moreover, absence of caspases (Olie *et al.*, 1998), an apoptotic cell death marker, makes this organism a good model system to study the mechanism of paraptotic cell death and the probable role of PARP. Studying PARP and cell death mechanisms in *D. discoideum* would throw light on the evolutionary aspects of programmed cell death (Mir *et al.*, 2007). We have earlier reported the high resistance of the unicellular stage of *D. discoideum* to oxidative stress (Katoch and Begum, 2003). The current study is an attempt to dissect out the key players during oxidative stress induced paraptotic and necrotic cell death in *D. discoideum*.

3.2. RESULTS

3.2.1. Induction of cell death in *D. discoideum* cells by oxidative stress

Experiments were designed to establish the ability of *D. discoideum* to undertake cell death as a function of oxidative stress. This was achieved by intracellular build up of H₂O₂ by hydroxylamine (HA) treatment or directly treating *D. discoideum* cells with cumene H₂O₂.

3.2.1.1. Intracellular build up of oxidative stress in *D. discoideum* cells

Cell death was induced by intracellular build up of H₂O₂. The cells were treated with different concentrations of HA (0, 1, 2.5, 3, 4 mM), a known inhibitor of catalase (Kono and Fridovich, 1983) leading to intracellular accumulation of ROS. HA induced cell death in *D. discoideum* was measured by the trypan blue exclusion method in a dose dependent manner. The percentage of *D. discoideum* cells undergoing death increased from 15% to 90% as HA levels increased from 1 to 4 mM, with incubation time of 12

hours (Fig. 3.1). Percent cell death remained same after a time interval of 12 hours and hence this time period is considered for further studies. The LD₅₀ i.e. the concentration of HA inducing about 50% cell death at 12 hours post treatment was found to be 2.5 mM.

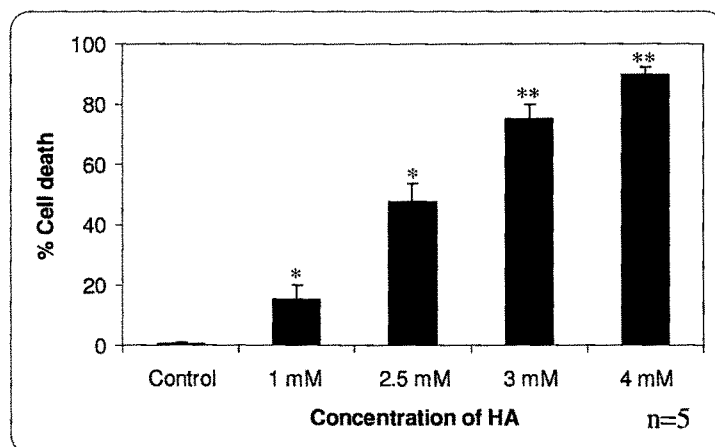


Figure 3.1: Oxidative stress (HA) induced dose dependent cell death as monitored by trypan blue exclusion method. Results are the mean \pm SE of five independent experiments. *** p value <0.001 ** p value <0.01, *p value <0.05 compared to control.

3.2.1.2. Induction of cell death in *D. discoideum* by exogenous addition of cumene H₂O₂:

Dose dependent induction of cell death in *D. discoideum* was studied by treating cells with cumene H₂O₂. In response to increasing doses of cumene H₂O₂ from 0.03 mM to 0.1 mM, the percentage of cells undergoing death were 15% and 90% respectively after 12 hours treatment regime, as examined by trypan blue exclusion (Fig. 3.2). The LD₅₀ was found to be 0.05 mM. Similar experiments were also done with cumene H₂O₂.

Staining with Annexin V-FITC in conjunction with vital dyes such as Propidium Iodide (PI) allows us to distinguish apoptotic cells (Annexin V positive, PI negative) from necrotic cells (Annexin V positive, PI positive). Thus, based on Annexin V-PI dual staining results, 2.5 mM HA and 0.05 mM cumene H₂O₂ doses were found to be necrotic as ~70% of the cells exhibited both PS exposure and PI staining at 3 hours (Fig. 3.3 B). In contrast, 1 mM HA and 0.03 mM cumene H₂O₂ were found to be paraptotic as PS exposure was exhibited by 50% cells after 5 hours while PI was not observed till 12 hours of oxidant treatment (Fig. 3.3A).

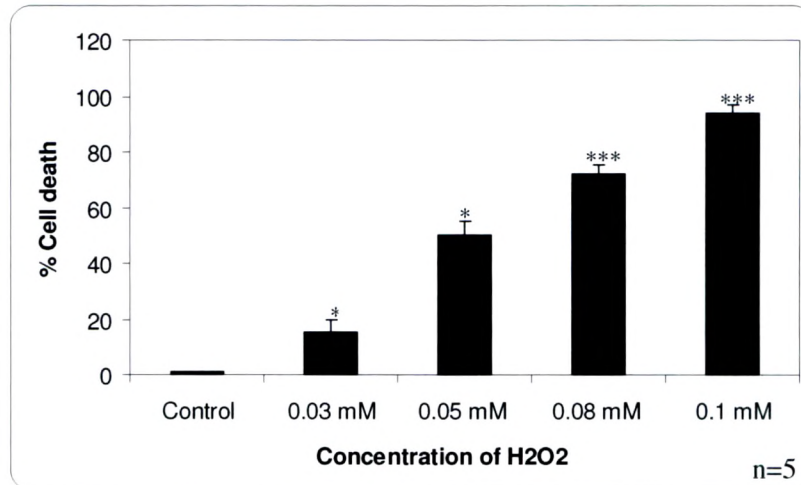


Figure 3.2: Oxidative stress (cumene H₂O₂) induces dose dependent cell death as monitored by trypan blue exclusion method. Dose dependent increase in cell death was observed with cumene H₂O₂. Results are the mean of five independent experiments \pm SE. ***p value <0.001, ** p value <0.01, * p value <0.05 compared to control.

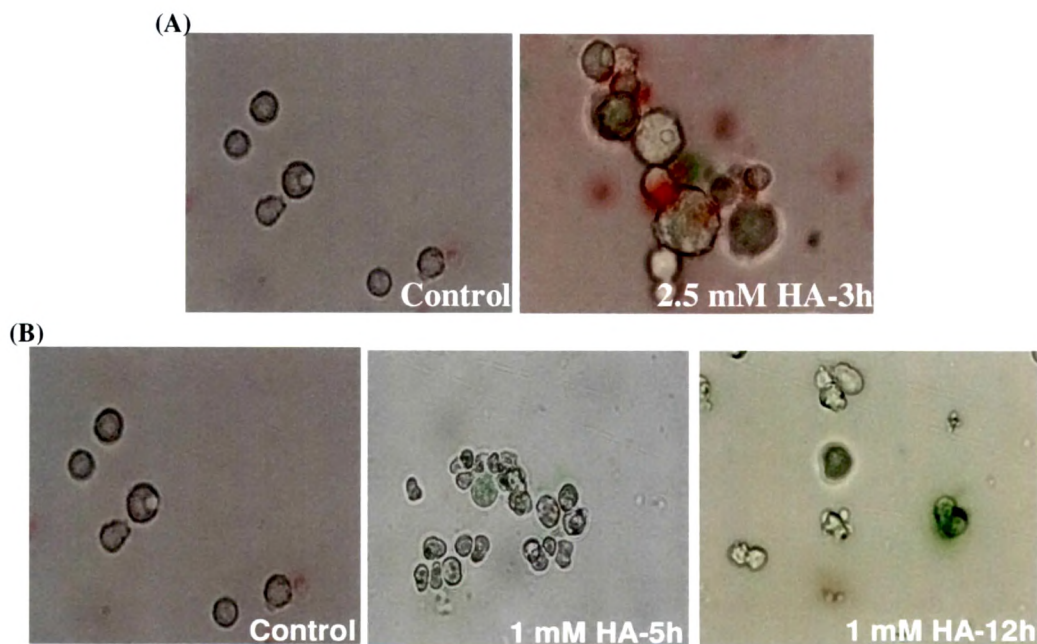


Figure 3.3: Annexin V staining of HA stressed *D. discoideum* cells. (A) 2.5 mM HA was found to be necrotic as both AnnexinV-FITC and PI staining were observed at 3 hours. (B) PS exposure is seen at 5 hours while PI staining at 12 hours with 1 mM HA. Data are representative of at least three independent experiments. Photographs were taken with 60X objective.

3.2.2. Measurement of Reactive Oxygen Species (ROS)

HA is known to generate *in situ* H₂O₂ and hence to confirm the production of H₂O₂, ROS levels were monitored. The amount of ROS produced was measured fluorimetrically with the DCFDA dye. Cells were harvested at 5 minutes post oxidant treatments (1 and 2.5 mM HA & 0.03 and 0.05 mM H₂O₂) for the estimation of intracellular ROS and the same was found to be increased in a dose dependent manner (Fig. 3.4).

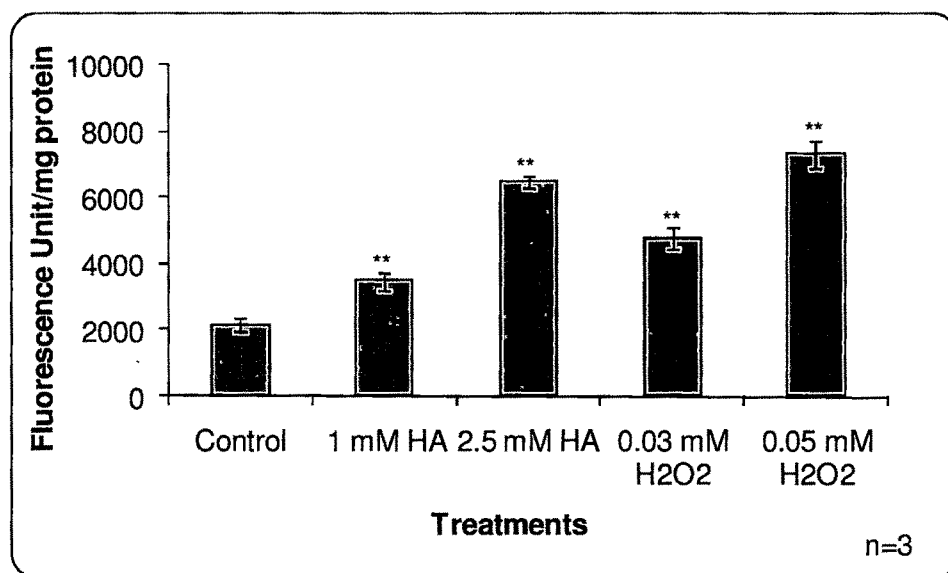


Figure 3.4: Fluorimetric estimation of ROS using DCFDA dye. ROS were measured at 5 minutes post oxidative stress. Data are represented as mean \pm S.E. from three independent experiments. ** p value <0.01, compared to control.

3.2.3. Oxidative stress mediated DNA damage

ROS generated during oxidative stress are known to cause DNA lesions; the most abundant being base modification and phosphorylation of gamma H2AX protein (Minami *et al.*, 2005). As our studies are based on PARP activation due to DNA damage we evaluated DNA damage caused by oxidative stress using antibody against H2AX phosphorylation. Our immunofluorescence microscopy results revealed that treatments with increasing doses of HA and cumene H₂O₂ resulted in increased H2AX phosphorylation within 5 minutes (Fig. 3.5).

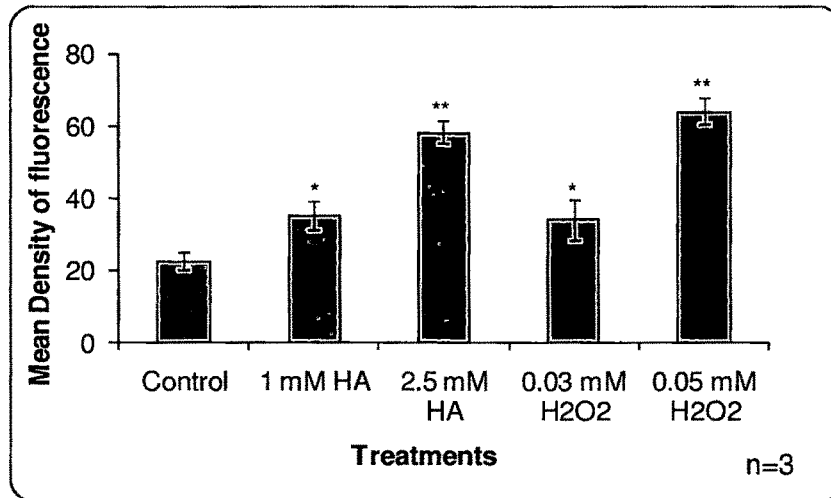


Figure 3.5: DNA damage induced by oxidative stress. DNA damage was observed 5 minutes post HA and cumene H₂O₂ stress by immunofluorescence using antibody against H2AX. Data (mean ± S.E.) are from three independent experiments. ** p value <0.01, * p value <0.05 as compared to control.

3.2.4. PARP activation induced by oxidative stress

Activation of PARP is seen in response to DNA damage. PARP activity in *D. discoideum* cells was assayed at various time points (5, 10, 20, 60 minutes and 4 hours) after oxidant treatment. PARP activity increased initially and peak activity was seen at 10 minutes post exposure to paraptotic doses of 1 mM HA or 0.03 mM cumene H₂O₂ (Fig. 3.6 A, 3.7 & 3.8). Results indicated no significant difference in PARP activity at 15 minutes time point after oxidant treatments. At necrotic doses, peak PARP activity was seen at 5 minutes post HA (2.5 mM) and cumene H₂O₂ treatments (0.05 mM) (Fig. 3.6 B, 3.7 & 3.8). High poly ADP-ribose levels were maintained for a few minutes and basal level was regained after 10 min of HA and H₂O₂ exposure during paraptosis (Fig. 3.6).

3.2.5. PARP inhibition delays oxidative stress induced cell death

To investigate whether the oxidative stress induced cell death in *D. discoideum* is PARP mediated, we pretreated the cells with PARP inhibitor benzamide prior to oxidative stress. Peak PARP activity which was observed at 10 minutes of 1 mM HA and 0.03 mM cumene H₂O₂ treatments, and 5 minutes of exposure to 2.5 mM HA and 0.05 mM cumene H₂O₂ was significantly inhibited by 1 mM benzamide (Figs. 3.9, 3.10 & 3.11). Benzamide alone also reduced the basal activity compared to control.

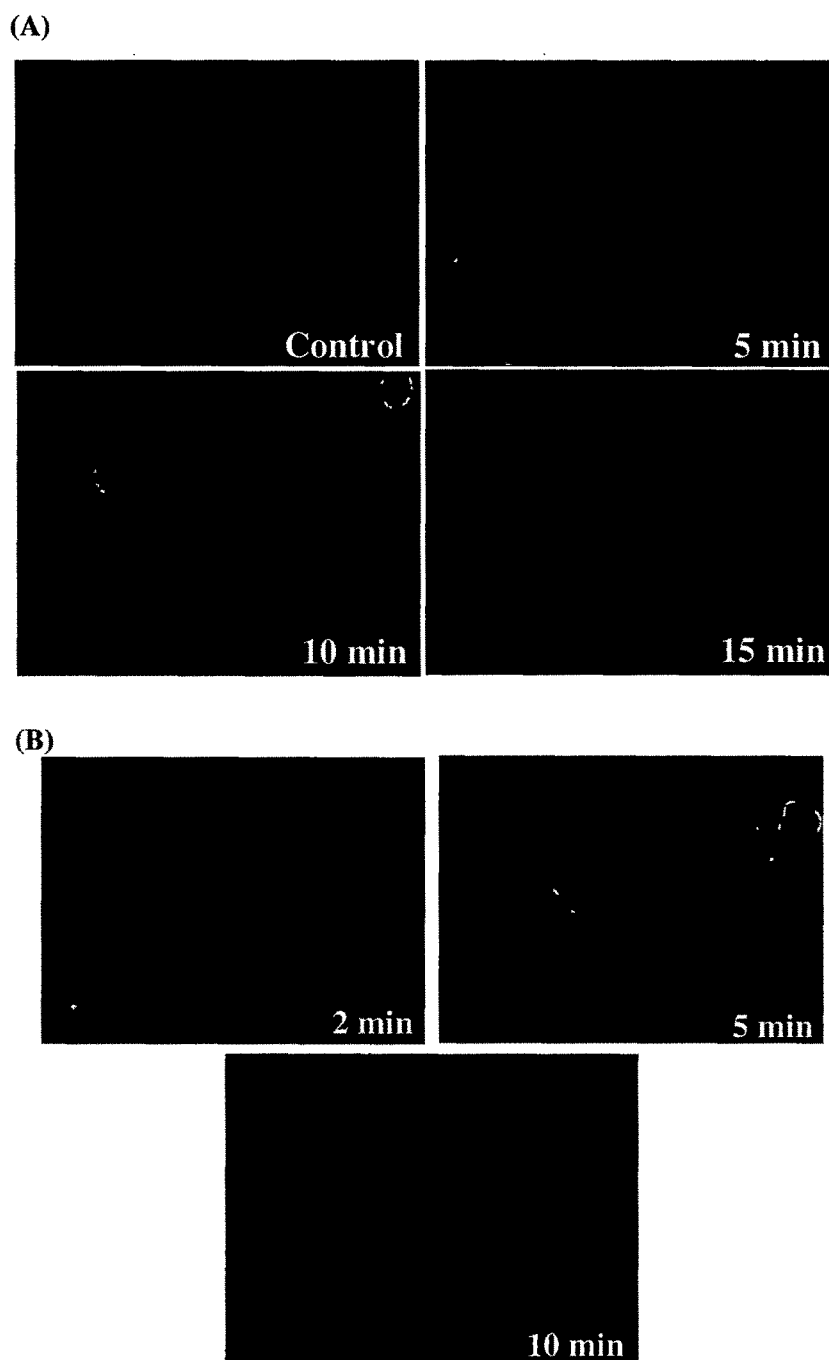


Figure 3.6: PARP activity assay by indirect immunofluorescence. (A) Under control conditions basal PARP activity was seen. Peak activity of PARP was seen at 10 minutes post 1 mM HA stress which reached basal level within 20 minutes. (B) Cells when treated with 2.5 mM HA showed increased PAR immunoreactivity at 5 minutes. Data are representative of at least five independent experiments. Photographs were taken with 60X objective.

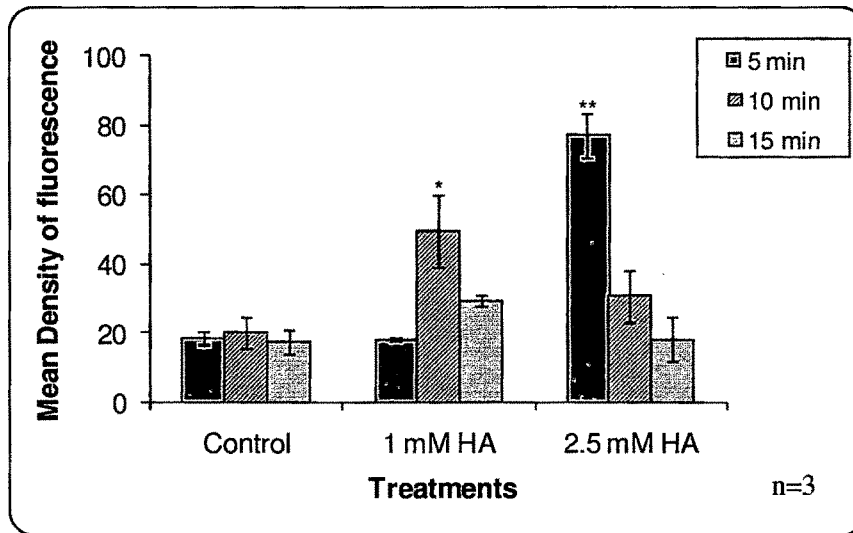


Figure 3.7: PARP activity assay by indirect immunofluorescence during HA stress. PARP activity was measured at different time points post HA stress. Peak activity was seen at 10 minutes post 1 mM HA and at 5 minutes post 2.5 mM HA stress. Data (mean \pm S.E.) are from five independent experiments. ** p value <0.01 , * p value <0.05 compared to control.

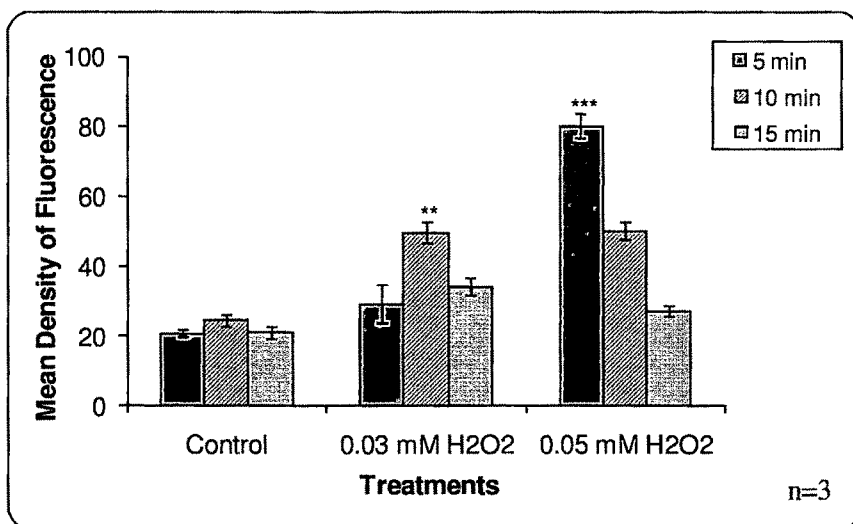


Figure 3.8: PARP activity assay by indirect immunofluorescence during cumene H₂O₂ stress. Peak PARP activity was observed at 10 minutes post 0.03 mM and at 5 minutes of 0.05 mM cumene H₂O₂ stress. Data (mean \pm S.E.) are from three independent experiments. *** p value <0.001 ; ** p value <0.01 compared to control.

(A)

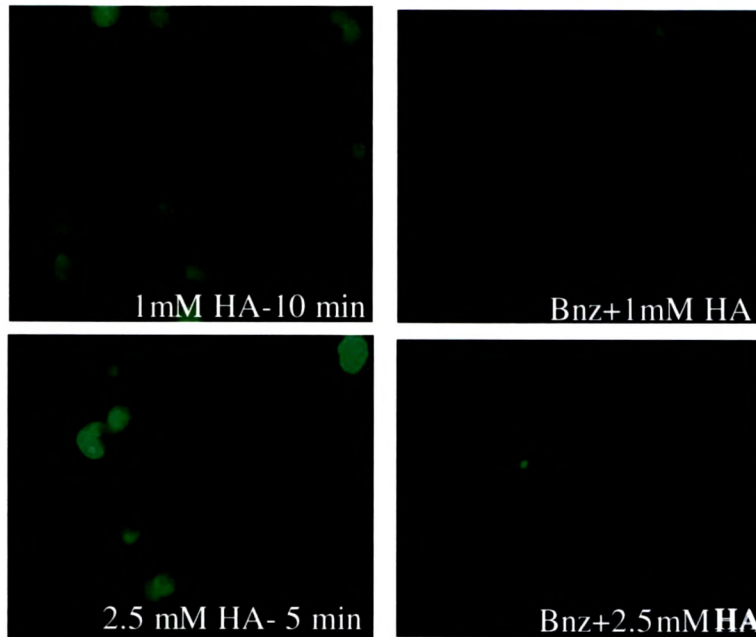


Figure 3.9: Peak PARP activity induced by HA was intercepted by benzamide. Benzamide inhibited PARP activity at 10 minutes and 5 minutes post 1 mM and 2.5 mM HA respectively.

(B)

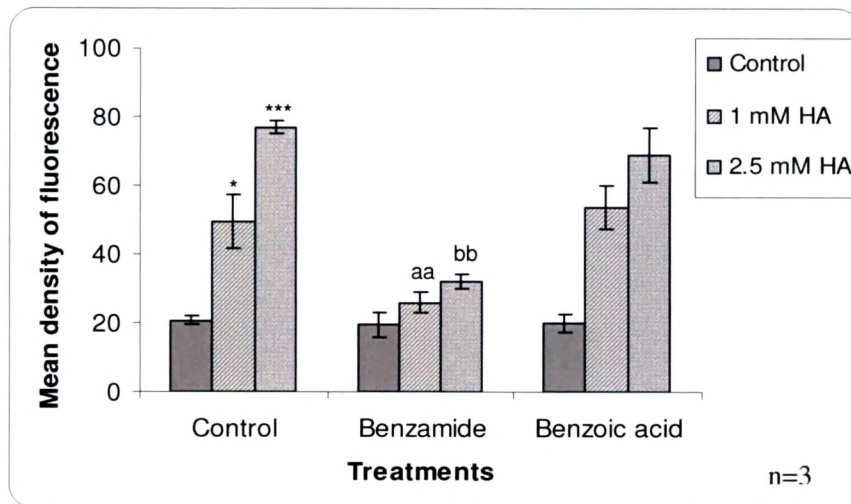


Figure 3.10: Densitometric analysis of PARP activity in presence of benzamide. Benzoic acid (BAC) is used as a structural analog of benzamide which did not show any effect on PARP activity. *** p value < 0.001, * p value < 0.05 compared to control; aa & bb p value < 0.01 compared to 1 mM HA and 2.5 mM HA respectively.

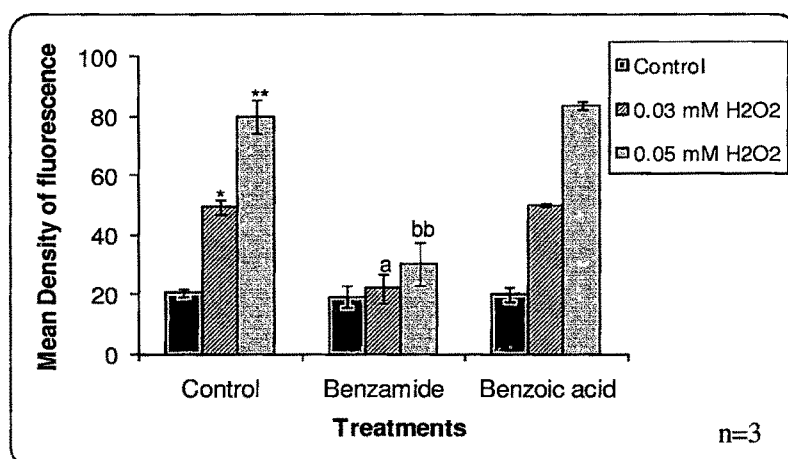


Figure 3.11: Peak PARP activity induced by cumene H₂O₂ was intercepted by benzamide. ** p value <0.01, * p value <0.05 compared to control; ^{bb} p value <0.01 compared to 0.03 mM H₂O₂; ^a p value <0.05 compared to 0.05 mM H₂O₂.

The cell death induced by HA and cumene H₂O₂ mediated oxidative stress was partially intercepted by benzamide (PARP inhibitor) as observed with trypan blue staining (Figs. 3.12 & 3.13). In PARP inhibited (benzamide pretreated) *D. discoideum* cells at 1 mM HA and 0.03 mM cumene H₂O₂ doses, PS exposure was seen at 12 hours and membrane integrity was not lost till 12 hours (Fig. 3.14). However at 2.5 mM HA and 0.05 mM cumene H₂O₂ doses PS was exposed at 3 hours and PI staining was seen at 6 hours (Fig. 3.14); suggesting that PARP inhibition delays paraptotic cell death and shifts necrosis to paraptosis.

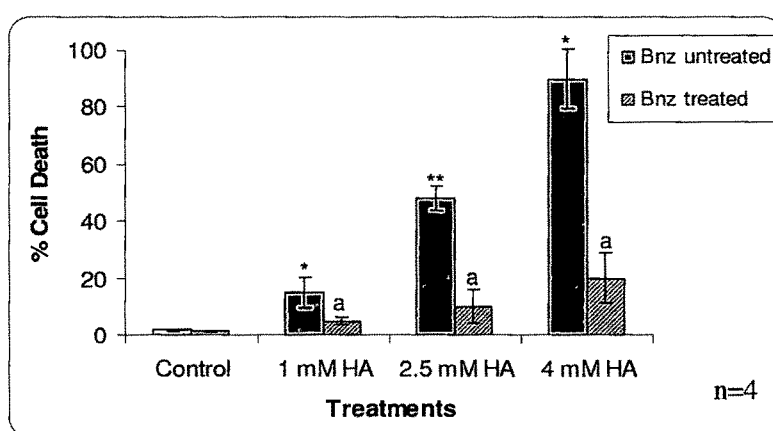


Figure 3.12: Effect of benzamide on HA induced cell death as monitored by trypan blue exclusion. Data (mean ± S.E.) are from three independent experiments. ** p value <0.01, * p value <0.05 compared to control, ^a p value <0.05 compared to respective treatments.

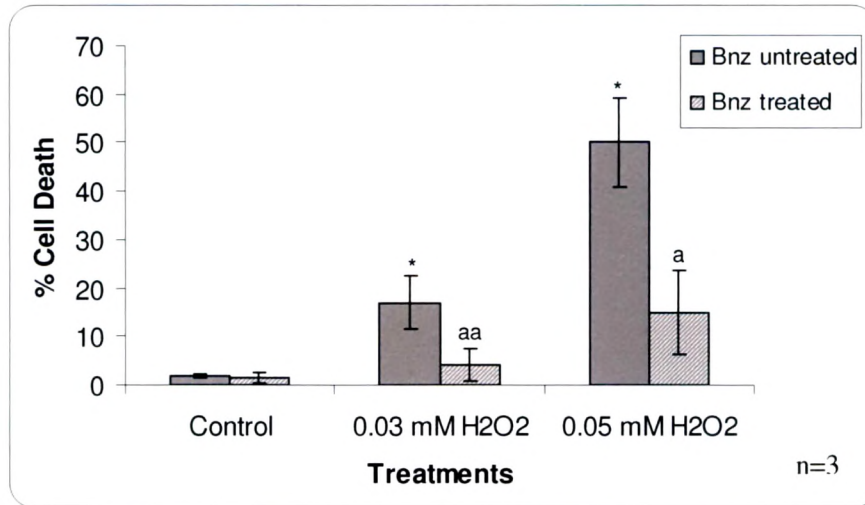


Figure 3.13: Effect of benzamide on cumene H₂O₂ induced cell death. Benzamide pretreatment partially prevented the cell death induced by cumene H₂O₂. Results are the mean of three independent experiments \pm SE. * p value <0.05 compared to control; aa p value <0.01, a = p value <0.05 compared to respective treatment.

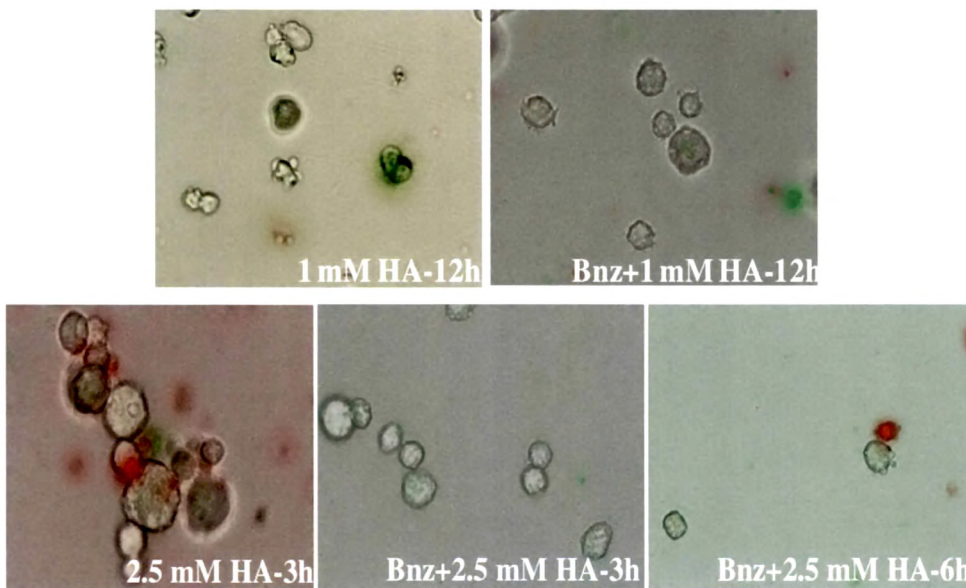


Figure 3.14: Effect of benzamide pretreatment on oxidative stress induced cell death. Data are representative of at least five independent experiments. Photographs were taken with 60X objective.

3.2.6. PARP activation leads to adenine and pyridine nucleotides depletion

PARP activation consumes cellular NAD^+ and ATP pools and depletion of adenine nucleotides offers one possible signal responsible for the downstream events in the paraptotic pathway. Thus PARP activation was also confirmed by monitoring cellular NAD^+ and ATP levels in control and HA treated cells and the results are shown in Figs. 3.15 and 3.16. NAD^+ and ATP contents were reduced to 60% and 45% of control values respectively within 1 hour of 1 mM HA treatment (Figs. 3.15 and 3.16). Additionally, 2.5 mM HA treated *D. discoideum* cells also exhibited a sharp decline (80% reduction) in NAD^+ and ATP levels within 1 hour of HA treatment (Figs. 3.15 and 3.16). These results support the early activation of PARP.

Our results on PARP inhibition with benzamide showed significant rescue in the depletion of cellular NAD^+ and ATP levels. 1 mM HA stressed cells with benzamide pretreatment could intercept the depletion in NAD^+ and ATP levels by 30% and 35% respectively. During necrosis (2.5 mM HA) PARP inhibition showed 45% rescue in ATP and 40 % rescue in NAD^+ (Figs. 3.15 and 3.16) levels, indicating that PARP activation caused reduction in cellular energy levels.

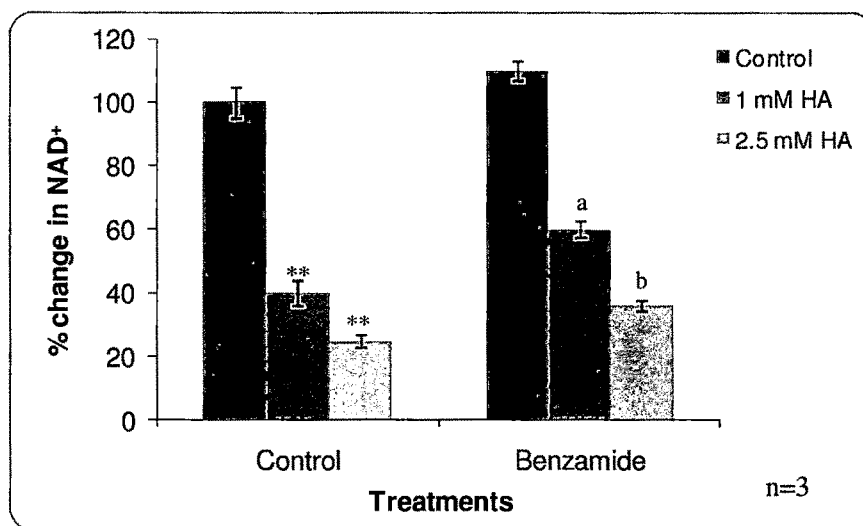


Figure 3.15: Oxidative stress depletes NAD^+ content of *D. discoideum* cells in a PARP dependent manner. ** p value <0.01 compared to control; a & b p value <0.05 compared to respective HA stress.

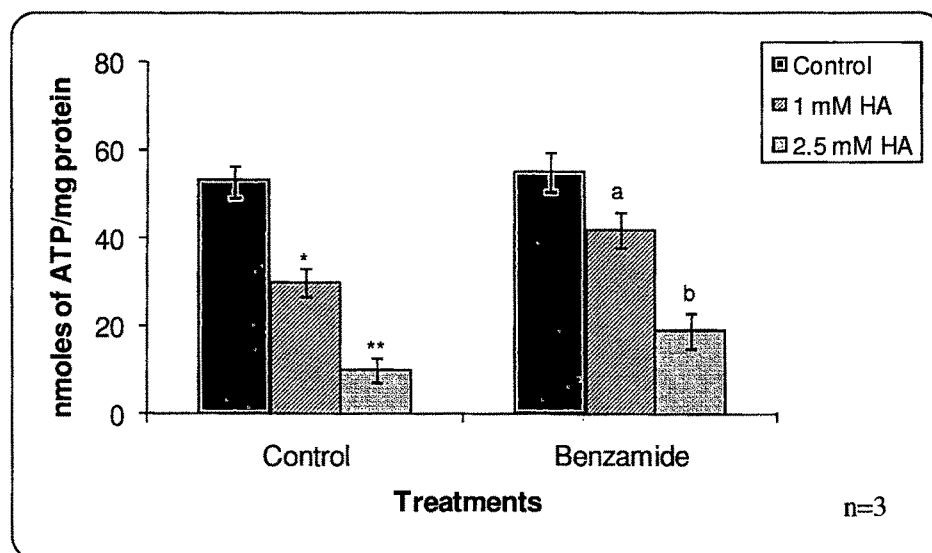


Figure 3.16: Oxidative stress depletes ATP content of *D. discoideum* cells in a PARP dependent manner. ** p value <0.01; * p value <0.05 compared to control; a & b p value <0.05 compared to respective HA stress.

3.2.7. Mitochondrial membrane potential (MMP) changes under oxidative stress

PARP dependent cell death was accompanied by changes in mitochondrial membrane potential. In order to determine the involvement of mitochondria in cell death we examined the changes in MMP using the membrane potential sensitive dye DiOC₆. Lower paraptotic doses led to an increase in MMP at an early stage. Nevertheless significant increase was observed in mitochondrial membrane potential in the initial phase of necrotic death (Fig. 3.17). Reduction in MMP was observed at 3 hours post 1 mM HA stress and complete loss occurred after 5 hours (Figs. 3.17 & 3.18). Similar results were obtained with 0.03 mM cumene H₂O₂ (Fig. 3.20). During necrosis (2.5 mM HA and 0.05 mM cumene H₂O₂) MMP was reduced in most of the cells by 2 hours (Figs. 3.19 & 3.20).

In accordance with nucleotide depletion results benzamide pretreatment also delayed MMP changes in cells exposed to 1 mM HA and 0.03 mM cumene H₂O₂ doses for 7 hours (Figs. 3.19 & 3.20), but it has no effect on MMP changes induced by 2.5 mM HA and 0.05 mM cumene H₂O₂ doses (Figs. 3.19 & 3.20).

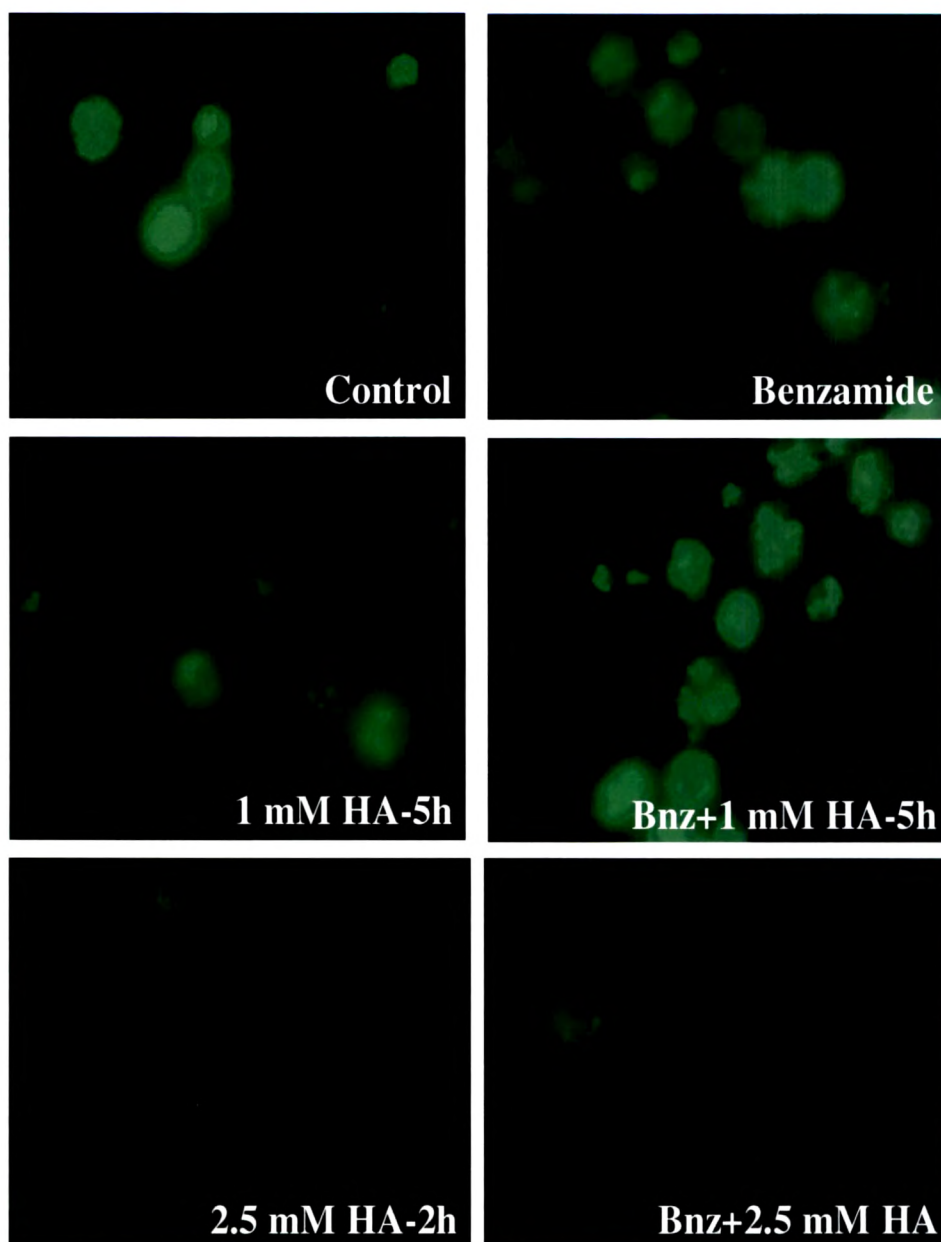


Figure 3.17: Mitochondrial membrane potential changes induced by oxidative stress. Live cells accumulate the dye in mitochondria so fluorescence intensity was found to be high in control and decreased with oxidative stress. Benzamide partially restored the changes in MMP. Data are representative of at least five independent experiments. Photographs were taken with 60X objective.

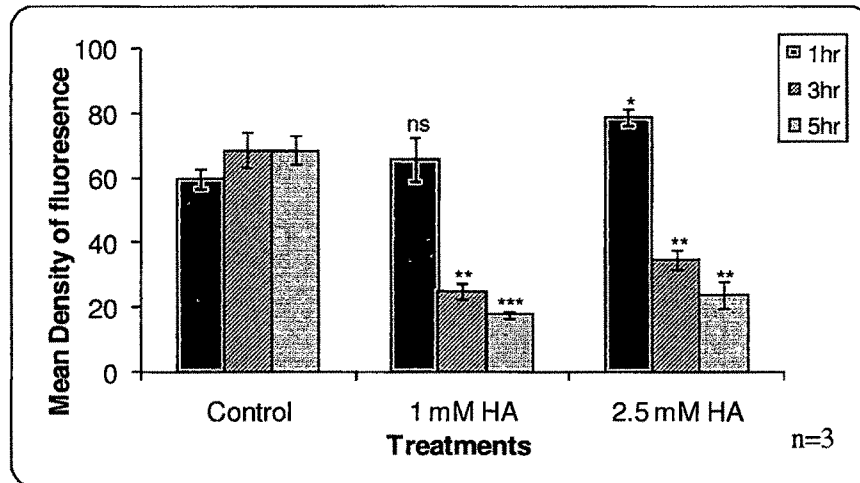


Figure 3.18: Time dependent changes in mitochondrial membrane potential after treatment with HA. Significant increase was found at 1 hour with necrotic dose. Following one hour MMP changes decreased significantly in both paraptotic and necrotic cell death. Results are the mean of three independent experiments \pm SE. *** p value <0.001 , ** p value <0.01 , * p value <0.05 compared to control.

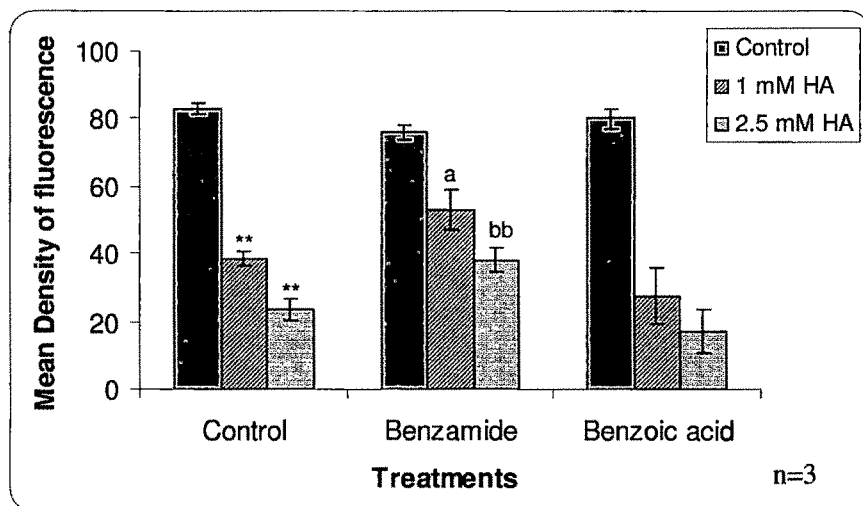


Figure 3.19: Changes in mitochondrial membrane potential after treatment with HA were partially rescued by benzamide. MMP change with 1 mM HA at 3 hours and 2.5 mM HA at 2 hours was partially restored by benzamide. Data (mean \pm S.E.) are from three independent experiments. ** p value <0.01 , compared to control; a, p value <0.05 compared to 1 mM HA; bb p value <0.01 compared to 2.5 mM HA.

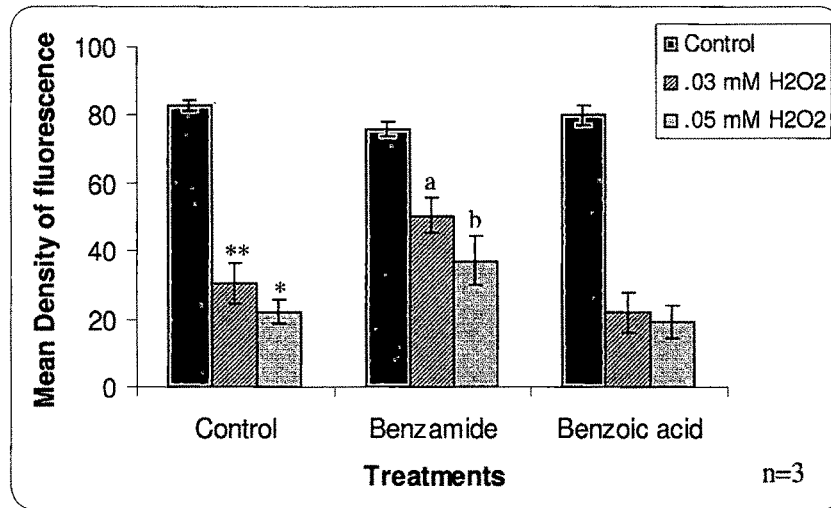


Figure 3.20: Changes in mitochondrial membrane potential after treatment with cumene H₂O₂ were partially rescued by benzamide. Results are the mean of three independent experiments \pm SE. ** p value <0.01, * p value <0.05 compared to control; a & b, p value <0.05 compared to respective H₂O₂ stress

3.2.8. AIF translocation is downstream to PARP activation

As Apoptosis inducing factor (AIF) translocation has been identified as a mediator of PARP induced cell death, we have monitored the release of AIF during HA induced cell death. AIF release under 1 mM HA dose was seen at 5 hours and its translocation to nucleus was observed by 6 hours (Fig. 3.21). These changes in the localization of AIF coincide with the MMP changes. During necrosis i.e., with 2.5 mM HA dose AIF release was seen by 2 hours (Fig. 3.21) along with MMP change.

PARP inhibition intercepted AIF release at 1 mM HA stress (Fig.3.21), however benzamide did not affect AIF translocation in 2.5 mM HA treated cells (Fig. 3.21).

3.2.9. Monitoring the release of cytochrome c from mitochondria

As *D. discoideum* exhibits caspase independent cell death, release of cytochrome c from mitochondria may not be of much significance. However we have observed the release of cytochrome c at 3 hours during *D. discoideum* paraptotic cell death (Fig. 3.22). Thus cytochrome c release could affect the functioning of mitochondria as it is coinciding with MMP changes and is upstream to Mitochondrial AIF release and further its translocation to the nucleus.

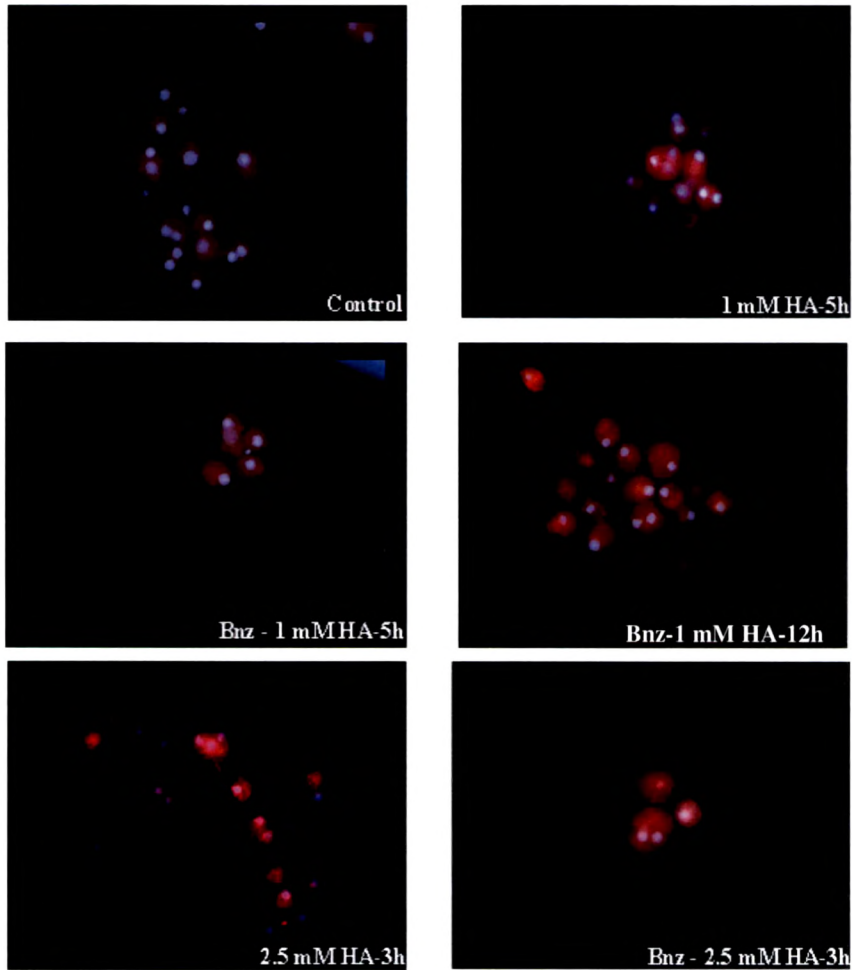


Figure 3.21: Fluorescence microscopy for the mitochondria-nuclear translocation of AIF. Data are representative of at least five independent experiments. Photographs were taken with 60X objective.

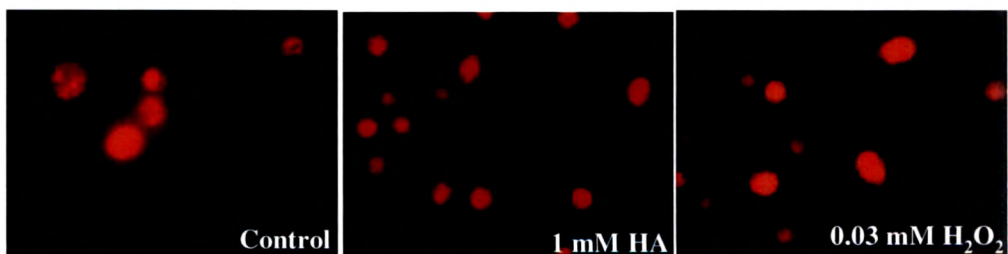


Figure 3.22: Cytochrome c release during paraptosis by immunofluorescence. Punctate staining in control cells indicate the localization of cyt c in mitochondria while diffused staining with HA and H_2O_2 indicate release of cyt c into cytosol at 3 hours. Data are representative of three independent experiments. Photographs were taken with 60X objective.

3.2.10. HA induced apoptosis leads to large scale DNA fragmentation

Oligonucleosomal DNA fragmentation is hallmark of apoptosis while paraptosis exhibits large scale DNA fragmentation. Such fragments cannot be resolved on agarose gel. DNA of *D. discoideum* cells exposed to 1 mM HA when subjected to agarose gel electrophoresis showed absence of oligonucleosomal DNA ladder (Fig. 3.23). However DNA fragmentation can be detected by TUNEL assay and a significant increase in TUNEL positive cells was seen (Fig. 3.24) at 6 hours post 1 mM HA stress suggesting that under oxidative stress *D. discoideum* cells undergo large scale DNA fragmentation. However, 2.5 mM HA and 0.05 mM H₂O₂ stressed cells exhibited DNA smear on agarose gel electrophoresis (Fig. 3.23) supporting the cell death to be of necrotic type. Thus these results reinforce that *D. discoideum* exhibits PARP mediated paraptosis and necrosis under low and high levels of oxidative stress respectively.

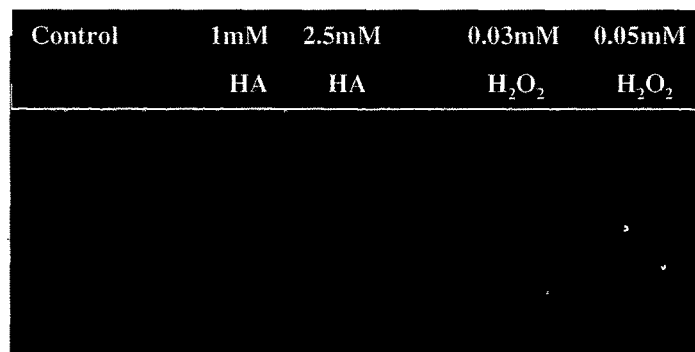


Figure 3.23: Monitoring DNA Fragmentation by Agarose gel electrophoresis. Figure shows the observed gel pattern from DNA isolated from Control and HA treated cells. No ladder formation is seen in 1 mM HA and 0.03 mM H₂O₂ treated cells.

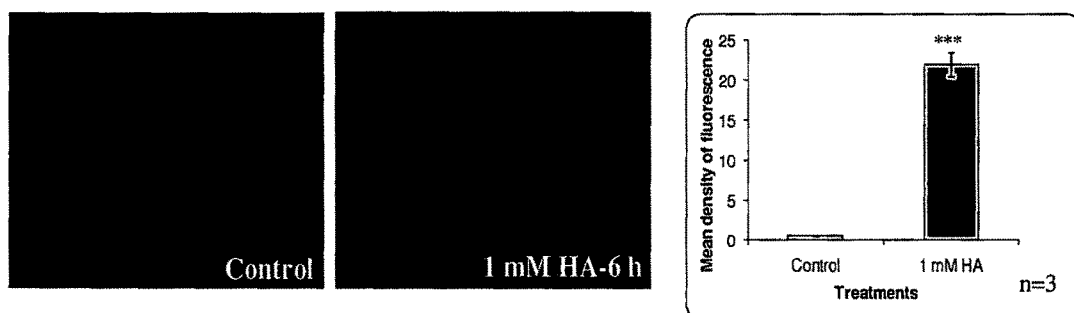


Figure 3.24: DNA fragmentation was monitored under oxidative stress using TUNEL assay. Results are the mean of three independent experiments \pm SE. *** p value <0.001 compared to control.

3.2.11. Oxidative stress induced cell death in *D. discoideum* is caspase independent

We have monitored caspase-3 activity during oxidative stress induced cell death. No significant change in caspase activity was seen in control and 1 mM HA stressed cells at 1 and 6 hours post stress. Caspase-3 specific inhibitor (DEVD-CHO) could not inhibit the observed caspase activity (Fig. 3.25), suggesting absence of caspase activation during oxidative stress induced paraptotic cell death in *D. discoideum*. 2.5 mM HA also exhibited non significant activity (Fig. 3.25).

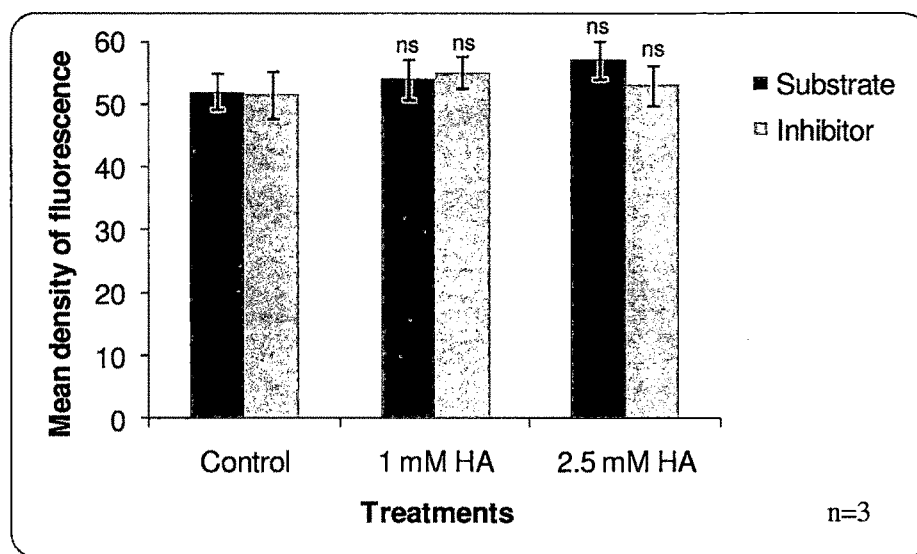


Figure 3.25: Caspase activity during paraptotic cell death. *D. discoideum* cells were treated with HA stress and caspase activity was assayed at 6 hours in form of DEVD-AMC cleavage and also in presence of caspase inhibitor. Caspase activity was non significant (ns).

3.2.12. Effect of broad caspase inhibitor on MMP changes and cell death

To demonstrate that the cytotoxicity effect is not due to caspase dependent pathway, cell death study was carried out with broad caspase inhibitor (zVAD-fmk). zVAD-fmk had no effect on MMP changes induced by oxidative stress and also on plasma membrane integrity as monitored by PI staining (Fig. 3.26 & 3.27). In the presence of 10 μ M zVAD-fmk, the cytotoxicity induced by oxidative stress was not inhibited indicating that *D. discoideum* cells take up caspase independent pathway. Further increasing the concentration of zVAD-fmk up to 25 μ M did not change our results.

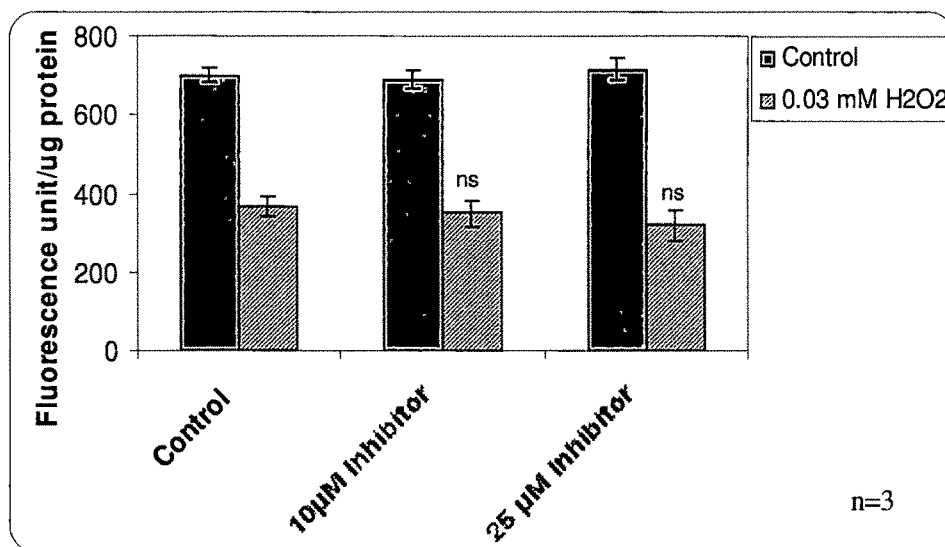


Figure 3.26: MMP changes in presence of broad caspase inhibitor during paraptosis. Data (mean \pm S.E.) are from three independent experiments. No significant (ns) effect was observed.

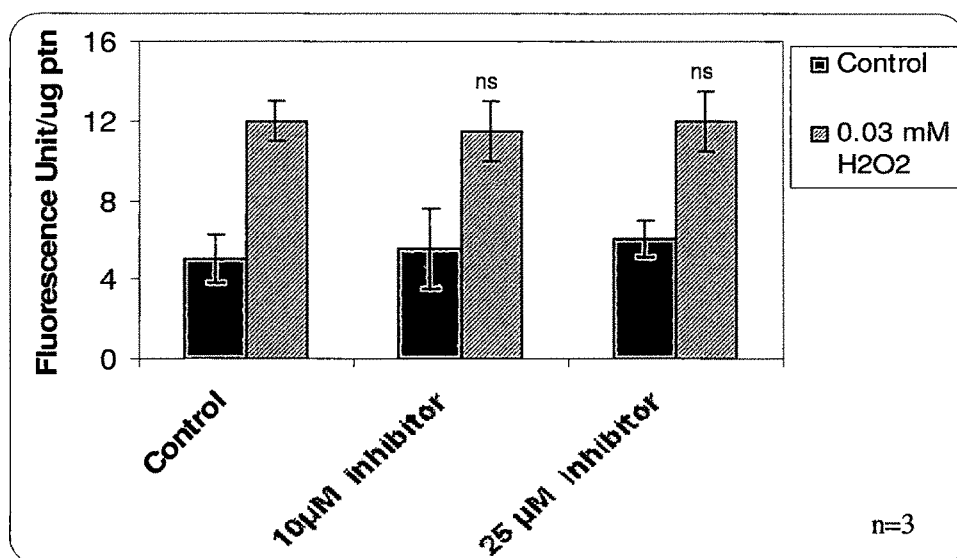


Figure 3.27: Propidium iodide staining in presence of broad caspase inhibitor during paraptosis. Data (mean \pm S.E.) are from three independent experiments.

3.2.13. Characterization of paraptotic vesicles

It would be of interest to examine the fate of dying paraptotic cells, whether they form paraptotic vesicles or not. We could observe the formation of vesicles at later stage after loss of plasma membrane integrity. Our results on biochemical characterization of the paraptotic vesicles formed under oxidative stress induced paraptotic cell death (1 mM HA) in *D. discoideum* suggest that the vesicles were membranous in nature (Figs. 3.28, 3.29) and contain DNA (Fig. 3.30). PS staining could not be seen suggesting that these vesicles did not exhibit PS exposure. Interestingly such vesicles were not observed with 2.5 mM HA stress.

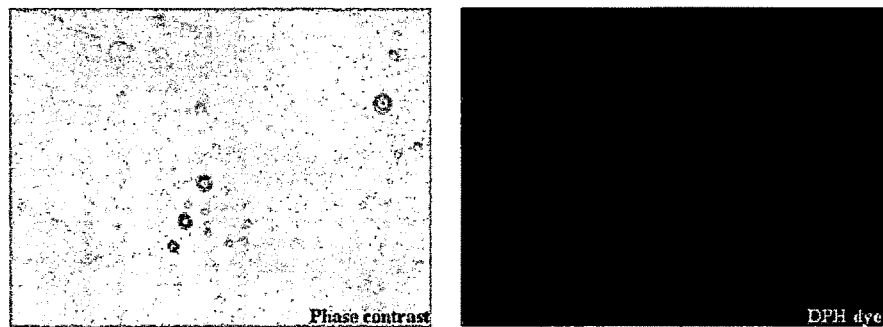


Figure 3.28: Paraptotic vesicle formation as seen by DPH staining. Data is representative of at least three independent experiments. Photographs were taken with 60X objective.

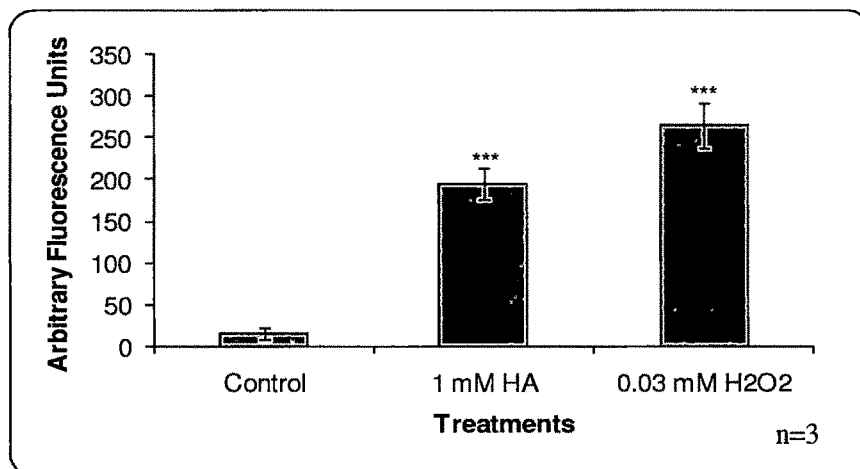


Figure 3.29: Characterization of paraptotic vesicles formed during oxidative stress using membrane probe DPH by fluorimetry. *** p value <0.001 compared to control.

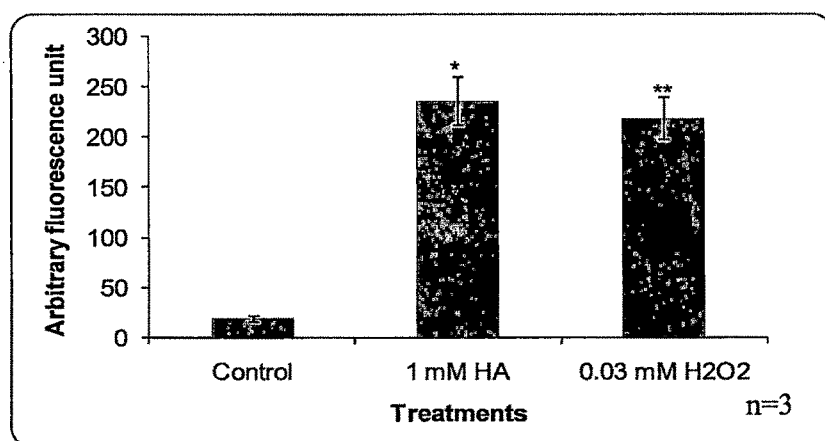


Figure 3.30: Characterization of paraptotic vesicles formed during oxidative stress using DNA binding dye DAPI. Data is representative of at least three independent experiment. ** p value <0.01, * p value <0.05 compared to control.

3.2.14. Effect of MEK inhibition on cell death

A recent report suggests the involvement of MAPK signaling in paraptosis (Sperandio *et al.*, 2004). To study the involvement of one of the MAP kinase kinase, MEK in oxidative stress induced cell death we inhibited MEK with its specific inhibitor (PD98059). To assess the dose dependent effect on cell death two different concentrations were used. MEK inhibition has affected oxidative stress induced MMP changes and also cell death. MMP changes at 3 hours were partially restored by higher dose of MEK inhibitor (Fig. 3.31). Both paraptotic and necrotic cell death was delayed with MEK inhibition (Fig. 3.32).

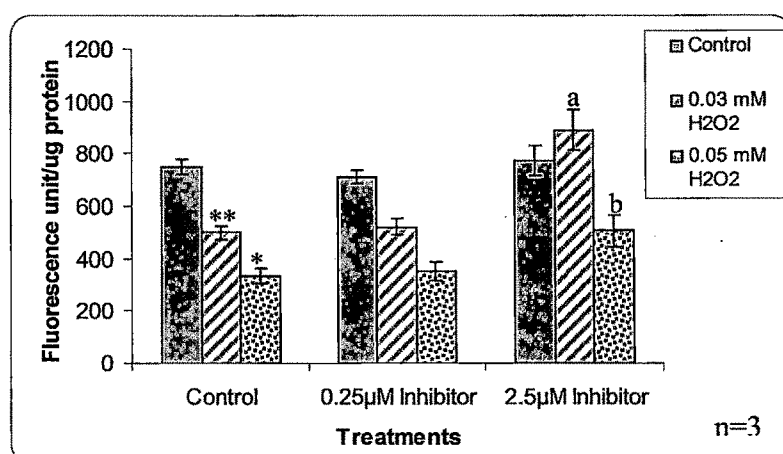


Figure 3.31: Oxidative stress induced MMP changes with MEK inhibition. Results are the mean of three independent experiments \pm SE. ** p value <0.01 compared to control; ^a & ^b p value <0.05 compared to respective H₂O₂ stress.

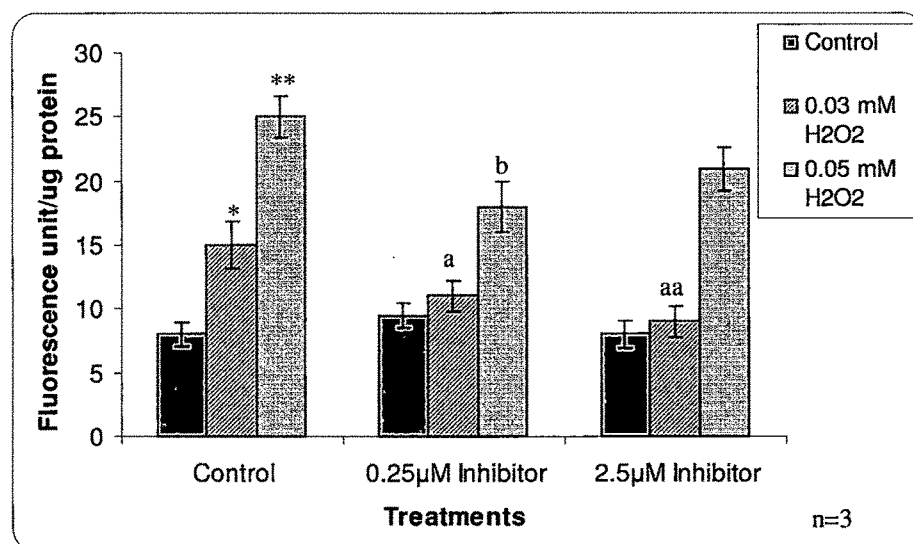


Figure 3.32: Propidium iodide staining to observe cell death upon MEK inhibition. Data (mean \pm S.E.) are from three independent experiments. ** p value <0.01, * p value <0.05 compared to control; aa p value <0.01 compared to 0.05 mM H₂O₂; a & b, p value <0.05 compared to respective H₂O₂ stress.

3.3. DISCUSSION

Cell death characterization

Programmed cell death may take the form of apoptotic or nonapoptotic types. While caspases mediate apoptosis, the mediators of nonapoptotic cell death programs are much less well characterized. Here, we report that paraptosis, an alternative, nonapoptotic cell death program that can be induced by oxidative stress, is mediated by PARP. This is supported by the observations that the PARP mediated paraptosis which occurs without caspase activation could be intercepted by the PARP inhibitor, benzamide. Also caspase inhibitors are found to be ineffective in blocking the cell death.

The present study demonstrates several important findings that help in understanding the sequence of events happening during oxidative stress induced PARP mediated *D. discoideum* cell death. Oxidative stress is a known inducer of cell death and severity of the stress determines whether cells undergo necrosis or apoptosis (Nosseri *et al.*, 1994; Palomba *et al.*, 1996). Dose dependent effect of hydroxylamine and cumene H₂O₂ was carried out to select paraptotic and necrotic doses, as *D. discoideum* did not

exhibit apoptosis due to absence of caspases (Olie *et al.*, 1998). Annexin V-FITC and PI dual staining results suggest that 2.5 mM HA and 0.05 mM cumene H₂O₂ doses were necrotic as both PS exposure and PI staining were seen simultaneously (Fig. 3.3A). Nevertheless, 1 mM HA and 0.03 mM cumene H₂O₂ stress yielded paraptotic cell death as PS exposure was visible at 5 hours post stress and plasma membrane integrity was lost after 12 hours (Fig. 3.3B). Thus, HA and cumene H₂O₂ at different concentrations can induce different types of cell death in *D. discoideum*. These results are parallel with a murine macrophage like tumor cell line which exhibited apoptosis and necrosis when exposed to lower and higher doses of H₂O₂ respectively (Schraufstatter *et al.*, 1986). Peroxynitrite was shown to trigger PARP dependent cell death in murine thymocytes (Virag *et al.*, 1998). Inhibition of poly(ADP-ribosylation) prevented intranuclear localization of apoptosis inducing factor and protected neurons from excitotoxic injury (Du *et al.*, 2003). Cell death induced by phagocyte derived oxygen radicals as well as exogenous hydrogen peroxide was efficiently prevented by PARP inhibitors (Thoren *et al.*, 2006).

Oxidative Stress and DNA damage

Oxidant imbalance in the cell leads to potential DNA damage. DNA bases are particularly susceptible to oxidation. The most abundant being base modification and phosphorylation of gamma H2AX protein (Minami *et al.*, 2005). Phosphorylation of H2AX (γ H2AX) at Ser139 is known to play a very early and important role in the cellular response to DNA double strand breaks and is mediated by ataxia telangiectasia mutated kinase (ATM) (Burma *et al.*, 2001; Sedelnikova *et al.*, 2003). Oxidative DNA damage was evaluated by monitoring the presence of histone H2AX phosphorylation. Within minutes following oxidative stress H2AX gets phosphorylated in *D. discoideum* cells as observed by immunofluorescence (Fig. 3.5).

PARP activation is the upstream event during paraptotic and necrotic cell death

Peak PARP activity was observed at 10 minutes of 1 mM HA treatment (Figs. 3.6 & 3.7) and 0.03 mM cumene H₂O₂ stress (Fig. 3.8) and at 5 minutes in 2.5 mM HA and 0.05 mM cumene H₂O₂ treated cells (Figs. 3.7 & 3.8). These results are consistent with those of Cipriani *et al.*, (2005) who demonstrated PARP activity under oxidative stress in

HeLa cells within 10 minutes. Pretreatment with benzamide resulted in inhibition of increased PARP activity at both the doses of HA and cumene H₂O₂ (Figs. 3.10 and 3.11).

As a consequence of PARP activation cellular NAD⁺ and ATP levels were reduced to 60% and 45% of control *D. discoideum* cells within 1 hour of 1 mM HA stress; and a reduction up to 80% in the cellular NAD⁺ and ATP levels was seen within 1 hour of 2.5 mM HA stress (Figs. 3.15 and 3.16). This reduction in the pyridine and adenine nucleotides is a supportive evidence for PARP activity as NAD⁺ serves as the substrate for PARP, and ATP is required for NAD⁺ replenishment (Kim *et al.*, 1994). NAD⁺ depletion is known to play an essential role in PARP mediated cell death (Alano *et al.*, 2004).

Cell death events occurring downstream to PARP activation

Several studies suggest that mitochondria play a central role in the execution of programmed cell death (Chandra *et al.*, 2002). Oxidative stress has been reported to cause mitochondrial dysfunction directly by promoting rapid loss of MMP (Cipriani *et al.*, 2005). When cells take up paraptosis, mitochondria undergo an initial priming phase associated with hyperpolarization which further leads to an effector phase, during which mitochondria swell and release proapoptotic proteins (Rego *et al.*, 2001). Subsequent to PARP activation mitochondrial membrane potential change was observed which increased (non significantly) initially at 1 hour, but reduced at 3 hours and was almost lost by 5 hours post 1 mM HA stress (Fig. 3.17 and 3.18). Conversely, in necrosis the MMP increased in 1 hour and then decreased at 2 hours post oxidative stress, much earlier compared to paraptotic dose (Fig. 3.17 and 3.18). With 0.03 mM cumene H₂O₂ loss in MMP was observed at 3 hours (Fig. 3.20). Increase in MMP observed in the initial phase could be due to shift in respiration from state 3 to state 4. Similar results were reported with HeLa cells upon exposure to MNNG (N-Methyl-N'-Nitro-N-Nitrosoguanidine). These cells exhibited an increase in MMP initially which was attributed to state 4 respiration due to ADP deficiency (Cipriani *et al.*, 2005). A decrease in state 3 respiration may be attributed to oxidative damage of the inner mitochondrial membrane or the mitochondrial complexes, which inhibits the electron transport and may increase membrane leakiness producing the enhanced state 4 respiration (Rego *et al.*, 2001).

MMP change leads to cytochrome c and AIF release which accounts for the nuclear changes (Daugas *et al.*, 2000). During paraptotic cell death downstream to MMP change, cytochrome c release was observed after 3 hours (Fig. 3.22) and AIF release was observed after 5 hours of oxidative stress (Fig. 3.21). However, the role of cytochrome c during paraptotic cell death is not yet known. Interestingly, AIF upon translocation to nucleus caused large scale DNA fragmentation at 6 hours (Fig. 3.23 & 3.24). During necrotic cell death nuclear translocation of AIF was observed at 3 hours (Fig. 3.21). Thus, like other cell death model systems *D. discoideum* cells also showed AIF translocation during paraptotic (Daugas *et al.*, 2000) and necrotic cell death (Moubarak *et al.*, 2007). However, the role of AIF in necrosis is not yet clear.

D. discoideum cells undergo paraptotic cell death in conditioned medium with the release of apoptotic vesicle like bodies characterized by the presence of DNA, protoporphyrin IX and phosphatidyl serine exposure (Arnoult *et al.*, 2001). Interestingly, *D. discoideum* exhibited paraptotic vesicle formation during oxidative stress induced paraptotic cell death. These vesicles consisted of DNA surrounded by a membrane as they were stained with DPH and DAPI (Fig. 3.28, 3.29 & 3.30) but did not contain protoporphyrin IX. However, vesicles were not detected during necrotic cell death.

Extent of PARP activation, energy derangement and the type of cell death

PARP is known to be activated rapidly in response to different DNA damaging agents and the type of cell death a cell exhibits depends on the extent of PARP activation in the nucleus (Chiarugi *et al.*, 2002; Hong *et al.*, 2004). To elucidate the role of PARP in different types of cell death under oxidative stress in *D. discoideum*, PARP inhibition studies were attempted by using benzamide, a known PARP inhibitor. In the presence of benzamide, paraptotic cell death was delayed by 7 hours and interestingly necrotic cell death was switched to paraptotic type (Fig. 3.14).

It is well documented that PARP inhibitors such as 3-aminobenzamide (3-AB) and nicotinamide or PARP-1 knockout can prevent energy depletion and hence increase viability of the cells exposed to oxidative stress (Schraufstatter *et al.*, 1986; Watson *et al.*, 1995). This cytoprotection is due to the prevention of NAD⁺ and ATP depletion caused by excessive PARP activation (Tapodi *et al.*, 2005). Our results showed that

pretreatment of *D. discoideum* cells with benzamide prevented the activation of PARP and rescued the NAD⁺ and ATP levels by ~30% and 35% respectively at paraptotic dose (Fig 3.15 & 3.16), thus maintaining the energy levels. This prevention in oxidative stress mediated alterations in energy levels by PARP inhibition indicates that PARP activation results in energy derangement. Our benzamide inhibition results were supported by PARP downregulation (Chapter 6).

Benzamide also partially prevented the loss of NAD⁺ and ATP during necrosis (Figs. 3.15 & 3.16). The data suggests that PARP inhibition resulted in partial recovery of ATP and hence shifts the mode of cell death to paraptotic type. Similar findings are reported in LLC-PK1 cells by Filipovic *et al.*, (1999). Thus the extent of PARP activation under different doses of oxidative stress affects the intracellular ATP levels, which further determines whether a cell would take up paraptotic or necrotic mode of cell death.

Mitochondrial changes

We have observed loss of MMP downstream to PARP activation during *D. discoideum* paraptotic cell death. Benzamide treatment delayed the change in MMP by 7 hours (Figs. 3.17 & 3.19) which correlates with the delay seen in PS exposure. Conversely, benzamide had no effect on MMP changes that occurred during necrotic cell death (Figs. 3.17, 3.19 & 3.20).

AIF is known to be an important executioner of caspase independent cell death. ROS mediated PARP activation is necessary for the AIF release from mitochondria (Kang *et al.*, 2004). PAR polymer itself or PARylated proteins or NAD⁺ depletion (Hong *et al.*, 2004) could lead to mitochondrial permeability transition, linking PARP activation to AIF translocation (Tapodi *et al.*, 2005). Our findings support this hypothesis as PARP inhibition partially prevented the release of AIF from mitochondria (Fig. 3.21) and also delayed DNA fragmentation (Fig.3.24).

Based on the results we have proposed a pathway which shows that paraptotic cell death is partially rescued by PARP inhibition (Fig. 3.33A) Benzamide is a potent rescuer of cell death induced by 1 mM HA and 0.03 mM cumene H₂O₂. Nevertheless, at

2.5 mM HA and 0.05 mM cumene H₂O₂ doses, inhibition of PARP hyperactivity switches the cell death to paraptotic type though some of the cell death parameters were not reversed (Fig. 3.33B) These results suggest that oxidative stress induced paraptosis is mediated by PARP and can be intercepted by benzamide.

It has been reported that paraptosis also can be seen in mammalian cells. Interestingly mammalian paraptosis is mediated by procaspase-9 wherein dominant negative mutant of procaspase-9 inhibited paraptosis. Procaspase-9 expression induced both apoptosis and paraptosis (Sperandio *et al.*, 2004). Paraptosis lacks many of the molecular and biochemical characteristics of apoptosis. Paraptosis and apoptosis represent two separate programs of cell death that are induced *via* distinct molecular pathways, but may be induced simultaneously by a single insult or agent. One feature distinguishing paraptotic cell death from apoptotic cell death is that paraptosis is not affected by broad caspase inhibitor (Fig. 3.26 & 3.27). In particular, apoptosis is inhibited by caspase inhibitors whereas paraptosis is resistant to such inhibitors. Involvement of procaspase-9 in paraptosis is independent of its proteolytic activity in the apoptotic pathway as evidenced by the resistance of paraptosis to Apaf-1. However, *D. discoideum* paraptosis may not be dependent even on procaspase function as this organism lacks caspases. Thus our results point out that paraptotic pathway could be further divided into procaspase-9 dependent and procaspase-9 independent types.

A striking similarity has been observed at the morphological level between paraptosis, type 3 (cytoplasmic) cell death, and the neuronal cell death observed in some neuro degeneration models, which suggests that paraptosis may be a physiologically relevant process. In order to assess its potential occurrence during development and in neurodegeneration, it will be necessary to identify specific markers for paraptosis, which are currently unavailable. It will also be important to characterize the molecular mechanisms underlying paraptosis to identify specific inhibitors for such nonapoptotic programmed cell death. These results support the concept that multiple, distinct cell death programs may be employed depending upon the stress condition and its severity. Oxidative stress generated by inhibiting intracellular GSH triggers the activation of various kinases like mitogen activated protein kinase (MAP kinase) and JNK in glial cells leading to Ca⁺² influx through TRMP (transient receptor potential protein,

melastatin subfamily) channels (Lee *et al.*, 2010). Another group has investigated the activation of MAP kinase in relation to cell death induced by peroxynitrite in human neuroblastoma SH-SY5Y cells. In such cells a selective inhibitor of MAP kinase kinase, reduced peroxynitrite induced cell death suggesting that activation of MAP kinase may be involved in cell death induced by peroxynitrite (Saeki *et al.*, 2000). Our results highlight the involvement of MEK in PARP mediated paraptotic cell death.

In conclusion, *D. discoideum* under mild (1 mM HA and 0.03 mM cumene H₂O₂) and moderate (2.5 mM HA and 0.05 mM cumene H₂O₂) conditions of oxidative stress exhibited PARP mediated paraptotic and necrotic cell death respectively. We have established *D. discoideum* as a model system for oxidative stress induced paraptotic and necrotic cell death, which can be extrapolated to higher eukaryotes. We have already reported the activation of PARP under oxidative stress in *D. discoideum* (Rajawat *et al.*, 2007). This is the first report where the downstream events after PARP activation during oxidative stress induced cell death in *D. discoideum*, an ancient eukaryote, are established. Our study suggests that paraptosis, an alternate cell death program may be regulated by the key players – PARP and AIF. Thus we have characterized the molecular mechanism underlying paraptosis that provides new insights to identify specific inhibitors for upstream mitochondrial events such as AIF translocation. This could be beneficial in the treatment of neurodegenerative and other diseases where cells take up paraptotic cell death.

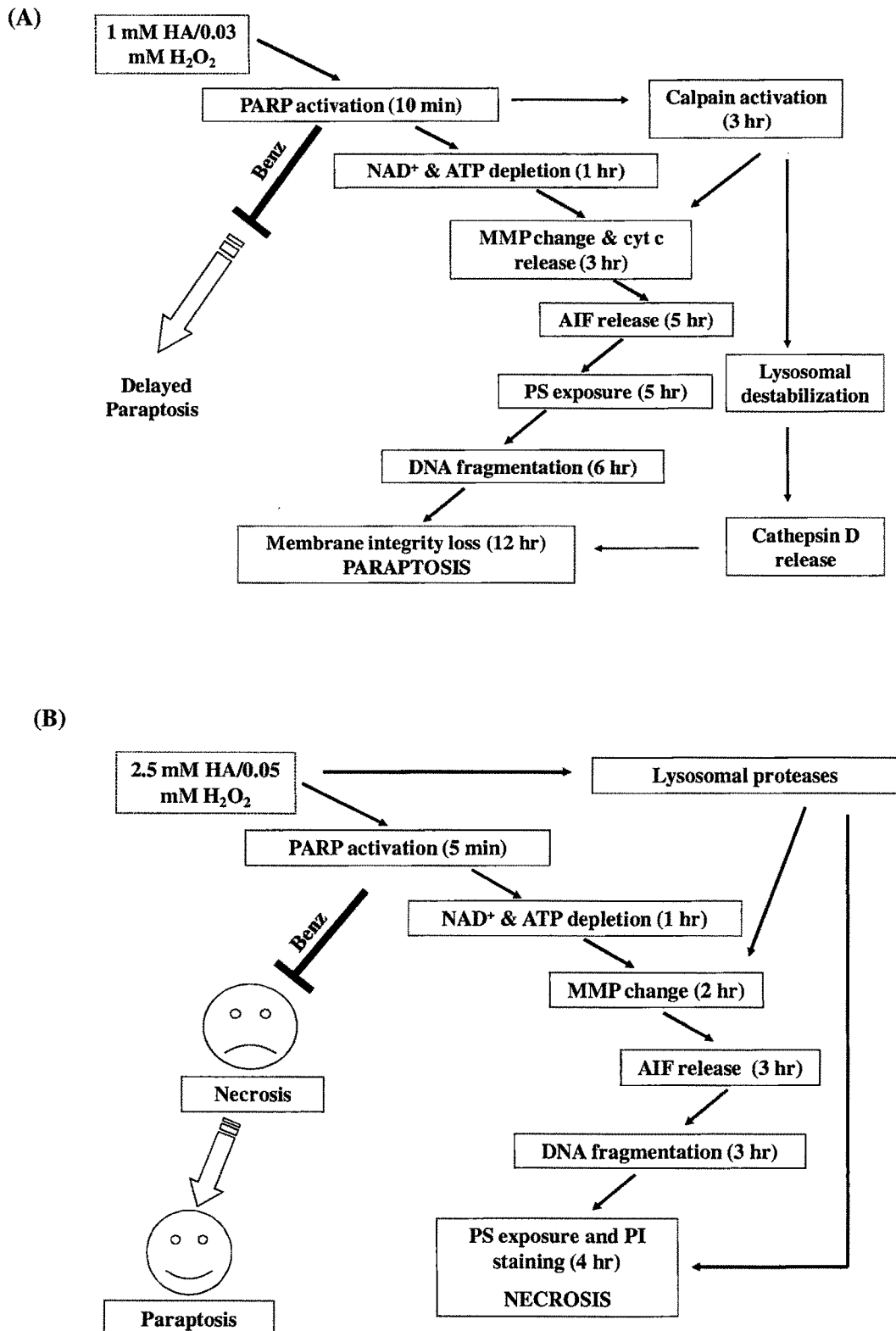


Figure 3.33: Proposed pathway for oxidative stress induced paraptosis and necrosis. Necrotic cell death switches to paraptotic type during PARP inhibition.

3.4. REFERENCES

- Alano C.C., Ying W. and Swanson R.A. Poly(ADP-ribose) polymerase-1 mediated cell death in astrocytes requires NAD⁺ depletion and mitochondrial permeability transition. (2004) *J. Biol. Chem.* 279, 18895-18902.
- Arnoult D., Tatischeff I., Estaquier J., Girard M., Sureau F., Tissier J.P., Grodet A., Dellinger M., Traincard F., Kahn A. et al. On the evolutionary conservation of the cell death pathway: mitochondrial release of an apoptosis-inducing factor during *Dictyostelium discoideum* cell death. (2001) *Mol. Biol. of Cell.* 12, 3016-3030.
- Burkley A. Physiology and pathophysiology of poly(ADP-ribosylation). (2001) *Bioessays.* 23, 795-806.
- Burma S., Chen B.P., Murphy M., Kurimasa A., Chen D.J. ATM phosphorylates histone H2AX in response to DNA double-strand breaks. (2001) *J. Biol. Chem.* 276, 42462-7.
- Chandra D., Liu J.W. and Tang D.G. Early mitochondrial activation and Cytochrome C up-regulation during apoptosis. (2002) *J. Biol. Chem.* 277, 50842-50854.
- Chiarugi A. Poly(ADP-ribose) polymerase: killer or conspirator? The 'suicide hypothesis' revisited. (2002) *Trends Pharmacol. Sci.* 23, 122-129.
- Ciprani H., Rapizzi E., Vannacci A., Rizzuto R., Moroni F. and Chiarugi A. Nuclear Poly(ADP-ribose) Polymerase-I rapidly triggers mitochondrial dysfunction. (2005) *J. Biol. Chem.* 280, 17227-17234.
- Daugas E., Susin S.A., Zamzami N., Ferri K.F., Irinopoulou T., Larochette N., Prevost M.C., Leber B., Andrews D., Penninger J. and Kroemer G. Mitochondrio-nuclear redistribution of AIF in apoptosis and necrosis. (2000) *FASEB J.* 14, 729-739.
- de Murcia G., Schreiber V., Molinete M., Saulier B., Poch O., Masson M., Niedergang C. and de Murcia M. Structure and function of Poly(ADP-ribose) polymerase. (1994) *Mol. Cell. Biochem.* 138, 15-24.
- Du L., Zhang X., Han Y.Y., Burke N.A., Kochanek P.M., Watkins S.C., Graham S.H., Carcillo J.A., Szabo C. and Clark R.S.B. Intra-mitochondrial Poly(ADP-ribosylation) contributes to NAD⁺ depletion and cell death induced by oxidative stress. (2003) *Journal of Biol. Chem.* 278, 18426-18433.

- Eliasson M.J.K., Sampei A.S., Mandir P.D., Hurn R.J., Traystman J., Bao A., Pieper Z.Q., Wang Q., Dawson T.M., Snyder S.H. and Dawson V.L. Poly(ADP-ribose) polymerase gene disruption renders mice resistant to cerebral ischemia. (1997) *Nat. Med.* 3, 1089-1095.
- Endres M., Wang Z.Q., Namura S., Waeber C. and Moskowitz M.A. Ischemic brain injury is mediated by the activation of Poly(ADP-ribose)polymerase. (1997) *J. Cereb. Blood Flow Metab.* 17, 1143-1151.
- Filipovic D.M., Meng X. and Reeves W.B. Inhibition of PARP prevents oxidant induced necrosis but not apoptosis in LLC-PK₁ cells. (1999) *Am. J. Physiol.* 46, 428-436.
- Fombonne J., Padron L., Enjalbert A., Krantic S. and Torriglia A. A novel paraptosis pathway involving LEI/L-DNaseII for EGF-induced cell death in somatotrope pituitary cells. (2006) *Apoptosis.* 11, 367-375.
- Haince J.F., Kozlov S., Dawson V.L., Dawson T.M., Hendzel M.J., Lavin M.F. and Poirier G.G. Ataxia telangiectasia mutated (ATM) signaling network is modulated by a novel poly(ADP-ribose)-dependent pathway in the early response to DNA-damaging agents. (2007) *J Biol Chem.* 282, 16441-16453.
- Hasnain S.E., Taneja T.K., Sah N.K., Mohan M., Pathak N., Sahdev S., Athar M. and Begum R. *in vitro* cultured *Spodoptera frugiperda* insect cells: Model for oxidative stress-induced apoptosis. (1999) *J. Biosci.* 24, 13-19.
- Hong S.K., Dawson T.M. and Dawson V.L. Nuclear and mitochondrial conversations in cell death: PARP-1 and AIF signaling. (2004) *Trends Pharmacol. Sci.* 23, 259-264.
- Joza N., Susin S.A., Daugas E., Stanford W.L., Cho S.K., Li C.Y.J., Sasaki T., Elia A.J., Cheng H.Y.M., Ravagnan L. et al. Essential role of the mitochondrial apoptosis inducing factor in programmed cell death. (2001) *Nature* .410, 549-554.
- Kang Y.H., Yi M.J., Kim M.J., Park M.T., Bae S., Kang C.M., Cho C.K., Park I.C., Park M.J., Rhee C.H. et al. Caspase-independent cell death by arsenic trioxide in human cervical cancer cells: reactive oxygen species-mediated Poly(ADP-ribose) Polymerase-1 activation signals apoptosis-inducing factor release from mitochondria. (2004) *Cancer research.* 64, 8960–8967.
- Katoch B. and Begum R. Biochemical basis of the high resistance to oxidative stress in *Dictyostelium discoideum*. (2003) *J. Biosci.* 28, 581-588.

- Katoch B., Sebastians S., Sahdev S., Padh H., Hasnain S.E. and Begum R. Programmed cell death and its clinical implications. (2002) *Indian J. Exp. Biol.* 40, 513-524.
- Kim H., Jacobson E.L. and Jacobson M.K. NAD Glycohydrolases: A possible function in calcium homeostasis. (1994) *Mol. Cell. Biochem.* 138, 237-243.
- Kono and Fridovich. Isolation and characterization of the pseudocatalase of *Lactobacillus plantarum*. (1983) *J. Biol. Chem.* 258, 6015-6019.
- Lautier D., Lagueux J., Thibodeau J., Menard L. and Poirier G.G. Molecular and biochemical features of poly (ADP-ribose) metabolism. (1993) *Mol. Cell. Biochem.* 122, 171-193.
- Lee M., Cho T., Jantaratnotai N., Wang Y.T., McGeer E. and McGeer P.L. Depletion of GSH in glial cells induces neurotoxicity: relevance to aging and degenerative neurological diseases. (2010) *FASEB Journal*.
- Lepretre C., Scovassi A.I., Shah G.M. and Torriglia A. Regulation of poly(ADP-ribose) polymerase-1 functions by leukocyte elastase inhibitor/LEI-derived DNase II during caspase-independent apoptosis. (2009) *Int J Biochem Cell Biol.* 41, 1046-54.
- Loeffler M., Daugas E., Susin S.A., Zamzami N., Metivier D., Nieminen A.L., Brothers G., Penninger J.M. and Kroemer G. Dominant cell death induction by extramitochondrially targeted apoptosis inducing factor. (2001) *FASEB J.* 15, 758-767.
- Minami T., Adachi M., Kawamura R., Zhang Y., Shinomura Y., and Imai K. Sulindac Enhances the Proteasome Inhibitor Bortezomib-Mediated Oxidative Stress and Anticancer Activity. (2005) *Clin Cancer Res.* 14, 11-17.
- Mir H., Rajawat J., Pradhan S. and Begum R. Signaling molecules involved in the transition of growth to development of *Dictyostelium discoideum*, (2007) *Indian J Exp. Biol.* 45, 223-236.
- Mohan M., Taneja T.K., Sahdev S., Krishnaveni M., Begum R., Athar M., Sah N.K. and Hasnain S.E. Antioxidants prevent UV-induced apoptosis by inhibiting mitochondrial cytochrome c release and caspase activation in *Spodoptera frugiperda* (Sf9) cells. (2003) *Cell Biol. Int.* 27, 483-490.
- Moubarak R.S., Yuste V.J., dric Artus C., da Bouharrou A., Greer P.A., de Murcia J.M. and Susin S.A. Sequential Activation of Poly(ADP-Ribose) Polymerase 1,

- Calpains, and Bax Is Essential in Apoptosis-Inducing Factor-Mediated Programmed Necrosis. (2007) *Mol. and Cell Biol.* 27, 4844–4862.
- Nosseri C., Coppola S. and Ghibelli L. Possible involvement of Poly(ADP-ribosyl) polymerase in triggering stress-induced apoptosis. (1994) *Exp. Cell Res.* 212, 367–373.
- Olie R.A., Durrieu F., Cornillon S., Loughran G., Gross J., Earnshaw W.C. and Golstein P. (1998) Apparent caspase independence of programmed cell death in *Dictyostelium*. *Current Biol.* 8, 955-958.
- Otto H., Reche P.A., Bazan F., Dittmar K., Haag F. and Koch-Nolte F. In silico characterization of the family of PARP-like Poly(ADP-ribosyl)transferases (pARTs). (2005) *BMC Genomics.* 6, 139-161.
- Palomba L., Sestili P., Cattabeni F., Azzi A. and Cantoni O. Prevention of necrosis and activation of apoptosis in oxidatively injured human myeloid leukemia U937 cells. (1996) *FEBS Lett.* 390, 91–94.
- Perkins E., Sun D., Nguyen A., Tulac S., Francesco M., Tavana H., Nguyen H., Tugendreich S., Barthmaier P., Couto J., Yeh E., Thode S., Jarnagin K., Jain A., Morgans D and Melese T. Novel inhibitors of poly(ADP-ribose) polymerase/PARP1 and PARP2 identified using a cell-based screen in yeast. (2001) *Cancer Res.* 15, 4175-83.
- Rajawat J., Vohra I., Mir H., Gohel D. and Begum R. Effect of oxidative stress and involvement of poly(ADP-ribose) polymerase (PARP) in *Dictyostelium discoideum* development. (2007) *FEBS J.* 274, 5611-5618.
- Raper K.B. *The Dictyostelids*, (1984) *Princeton University Press, Princeton, NJ* 453.
- Rego A.C., Vesce S. and Nicholls D.G. The mechanism of mitochondrial membrane potential retention following release of cytochrome c in apoptotic GT1-7 neural cells. (2001) *Cell Death and Diff.* 8, 995 – 1003.
- Saeki M., Kamisaki Y., Maeda S. Involvement of mitogen-activated protein kinase in peroxynitrite-induced cell death of human neuroblastoma SH-SY5Y cells. (2000) *Neurosci. Res.* 38, 213-216.
- Sah N.K., Taneja T.K., Pathak N., Begum R., Athar M. and Hasnain S.E. The baculovirus antiapoptotic p35 gene also functions via an oxidant-dependent pathway. (1999) *Proc. Natl. Acad. Sci.* 96, 4838-4843.

- Schraufstatter I.U., Hyslop P.A., Hinshaw D.B., Spragg R.G., Sklar L.A. and Cochrane C.G. Hydrogen peroxide-induced injury of cells and its prevention by inhibitors of Poly(ADP-ribose) polymerase. (1986) *Proc. Natl. Acad. Sci.* 83, 4908–4912.
- Sedelnikova O.A., Pilch D.R., Redon C. and Bonner W.M. Histone H2AX in DNA damage and repair. (2003) *Cancer Biol. Ther.* 2, 233-235.
- Shall S. and de Murcia G. Poly(ADP-ribose) polymerase-1: what have we learned from the deficient mouse model? (2000) *Mutat. Res.* 460, 1-15.
- Smulson M.E., Simbulan-Rosenthal C.M. and Boulares A.H. Roles of Poly(ADP-ribose)ylation and PARP in apoptosis, DNA repair, genomic stability and functions of p53 and E2F-1. (2000) *Adv. Enzyme regul.* 40, 183-215.
- Sperandio S., de Belle I. and Bredesen D.E. An alternative, nonapoptotic form of programmed cell death. (2000) *Proc. Natl. Acad. Sci.* 97, 14376-14381.
- Sperandio S., Poksay K., de Belle I., Lafuente M.J., Liu., Nasir J. and Bredesen D.E. Paraptosis: mediation by MAP kinases and inhibition by AIP-1/Alix. (2004) *Cell Death and Diff.* 11, 1066–1075.
- Susin S.A., Lorenzo H.K., Zamzami N., Marzo I., Snow B.E., Brothers G.M., Mangion J., Jacotot E., Costantini P., Loeffler M. et al. Molecular characterization of mitochondrial apoptosis-inducing factor. (1999) *Nature.* 397, 441-446.
- Szabo C. and Dawson V.L. Role of Poly(ADP-ribose) synthetase in inflammation and ischaemia-reperfusion. (1998) *Trends Pharmacol. Sci.* 19, 287–298.
- Tapodi A., Debreceni B., Hanto K., Bogнар Z., Wittmann I., Gallyas F., Varbiro G. and Sumegi B. Pivotal role of Akt activation in mitochondrial protection and cell survival by Poly(ADP-ribose) polymerase-1 inhibition in oxidative stress. (2005) *J. Biol. Chem.* 280, 35767-35775.
- Thoren F.B., Romero A.I. and Hellstrand K. Oxygen radicals induce Poly(ADP-Ribose) Polymerase-dependent cell death in cytotoxic lymphocytes1. (2006) *Journal of Immunol.* 176, 7301-7307.
- Virag L. PARP-1 and the shape of cell death. (2006) *Springer Sciences* 141-152.
- Virag, L., G. S. Scott, S. Cuzzocrea, D. Marmer, A. L. Salzman, and C. Szabo. Peroxynitrite-induced thymocyte apoptosis: the role of caspases and poly (ADP-ribose) synthetase (PARS) activation. (1998) *Immunology* 94, 345–355.

-
- Wang Y., Li X., Wang L., Ding P., Zhang Y., Han W. and Ma D. An alternative form of paraptosis-like cell death, triggered by TAJ/TROY and enhanced by PDCD5 overexpression. (2003) *Journal of Cell Sci.* 117, 1525-1532.
- Wang Y., Li X., Wang L., Ding P., Zhang Y., Han W. and Ma D. Apoptosis-inducing factor substitutes for caspase executioners in NMDA-triggered excitotoxic neuronal death. (2004) *J. Cell Sci.* 117, 1525-1532.
- Watson A.J., Askew J.N. and Benson R.S. Poly (adenosine diphosphate ribose) polymerase inhibition prevents necrosis induced by H₂O₂ but not apoptosis. (1995) *Gastroenterology.* 109, 472–482.
- Wyllie and Golstein. More than one way to go. (2001) *Proc. Natl. Acad. Sci.* 98, 11-13.